

Structure and optical properties of $\text{Ag}_{135}\text{Cu}_{60}$ nanocluster incorporating an Ag_{135} fullerene wrapped by copper complexes

Li Tang,^{1,2,4} Weinan Dong,^{3,4} Qikai Han,^{2,4} Bin Wang,² Zhennan Wu,^{3,*} Shuxin Wang^{1,2,*}

¹ Key Laboratory of Optic-Electric Sensing and Analytical Chemistry for Life Science, MOE, College of Chemistry and Molecular Engineering, Qingdao University of Science and Technology, Qingdao 266042, P. R. China.

² College of Materials Science and Engineering, Qingdao University of Science and Technology, Qingdao 266042, P. R. China.

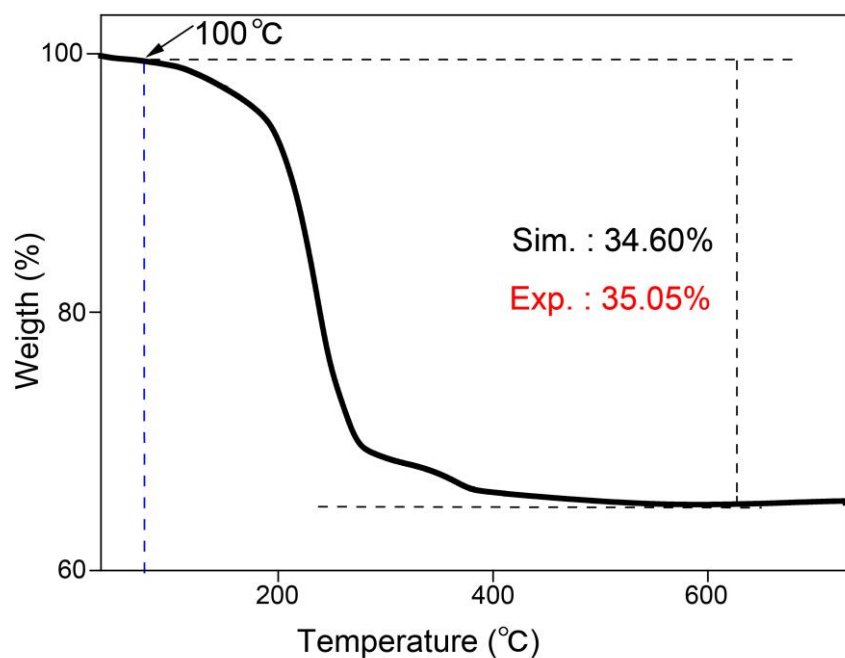
³ State Key Laboratory of Integrated Optoelectronics, College of Electronic Science and Engineering, Jilin University, Changchun, 130012, China.

⁴ These authors contributed equally: Li Tang, Weinan Dong, Qikai Han

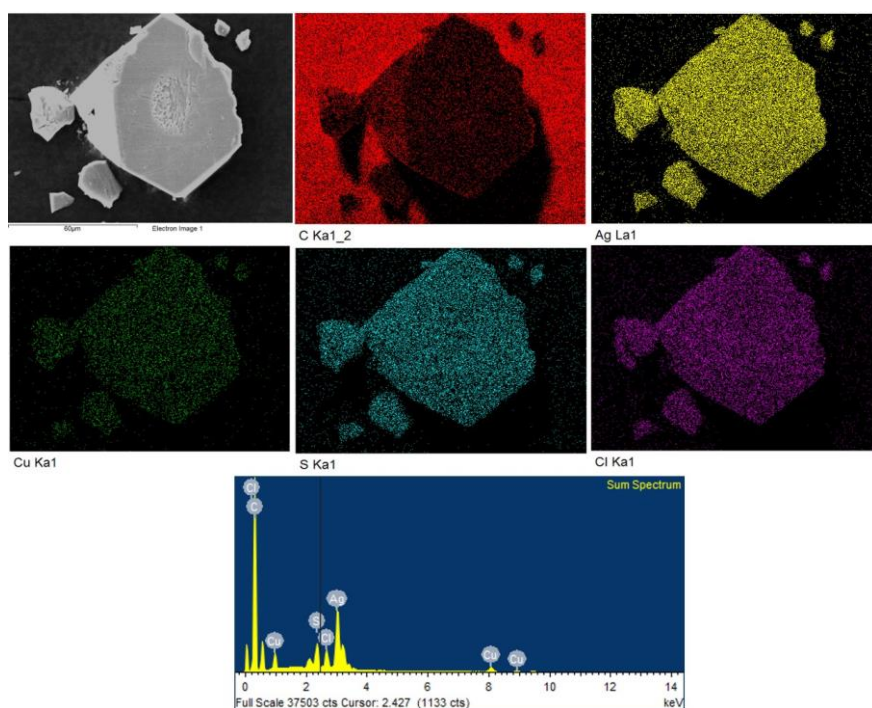
This PDF file includes:

| | |
|-----------------------------------------------------------------------------------------------|----|
| Supplementary Figures 1-22..... | 2 |
| Supplementary Tables 1-6..... | 14 |
| ORTEP view of $\text{Ag}_{135}\text{Cu}_{60}$ nanocluster | 17 |
| Explanations for A and B alerts in $\text{Ag}_{135}\text{Cu}_{60}$ nanocluster structure..... | 18 |

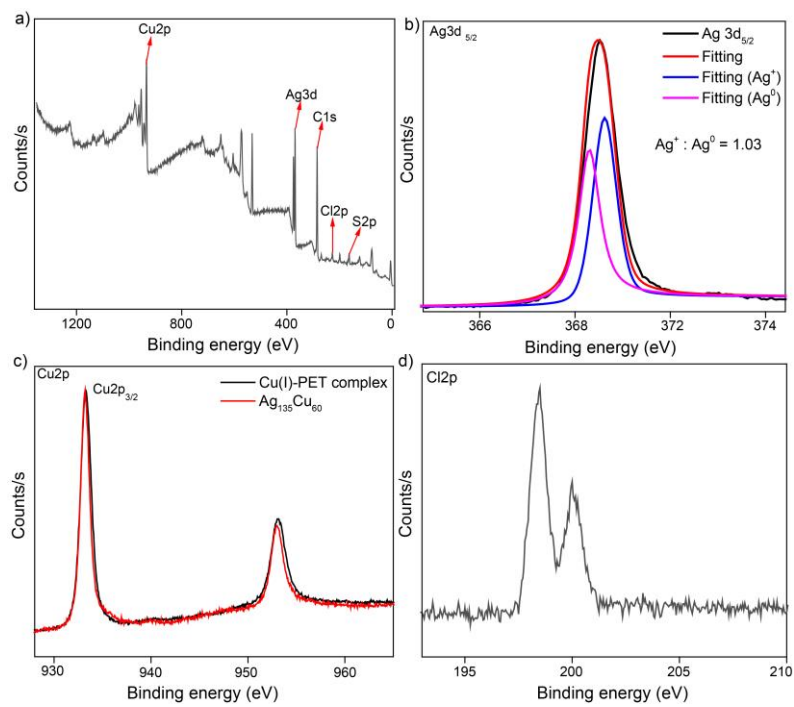
Supplementary Figures 1-22



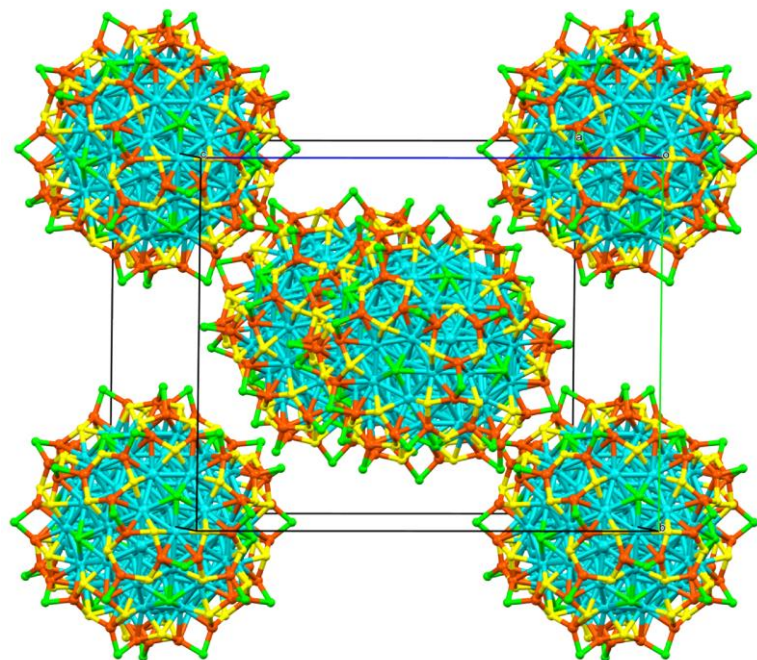
Supplementary Fig. 1. Thermogravimetric analyses (TGA) curves of $\text{Ag}_{135}\text{Cu}_{60}$ in N_2 atmosphere. Thermogravimetric analyses (TGA) revealed that $\text{Ag}_{135}\text{Cu}_{60}$ was stable until 100 °C.



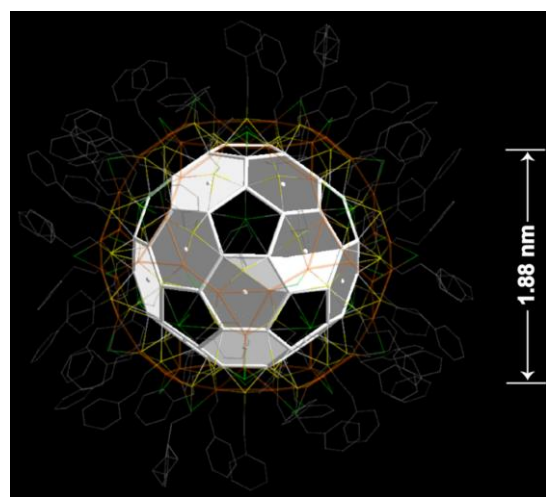
Supplementary Fig. 2 Elemental mapping images and energy dispersive spectrometer (EDX) analysis of the $\text{Ag}_{135}\text{Cu}_{60}$ nanocluster crystal.



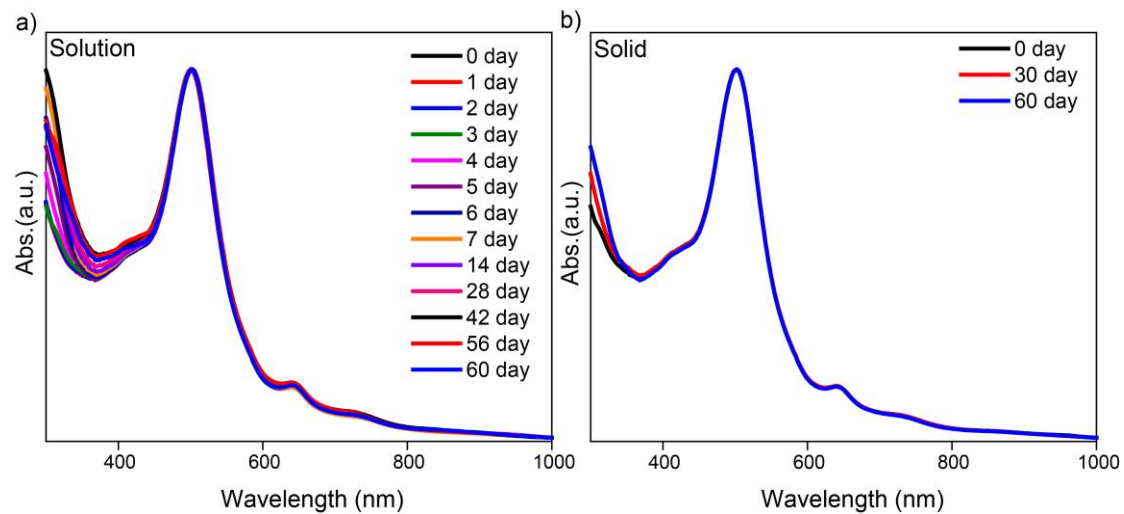
Supplementary Fig. 3. X-ray photoelectron spectroscopy (XPS) of $\text{Ag}_{135}\text{Cu}_{60}$ nanocluster. (a) XPS, (b) Ag 3d, (c) Cu2p. (d) Cl. Counts/s



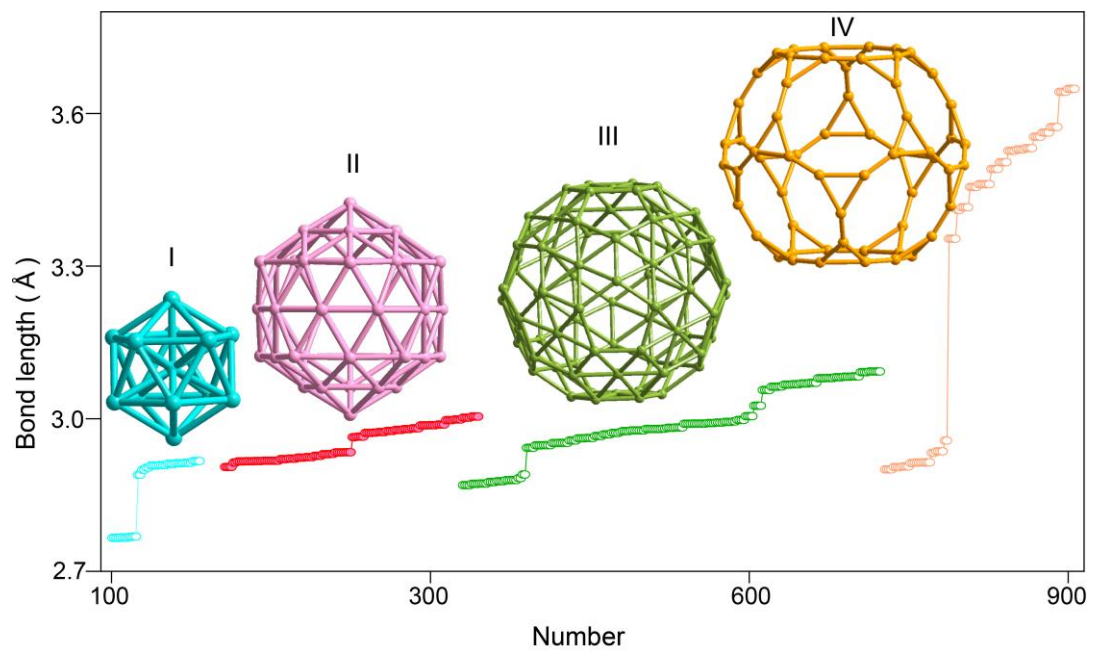
Supplementary Fig. 4. The unit cell of the crystal of the $\text{Ag}_{135}\text{Cu}_{60}(\text{SR})_{60}\text{Cl}_{42}$ nanocluster. Color labels: turquoise = Ag; orange = Cu; yellow = S; green = Cl. All C and H atoms were omitted for clarity.



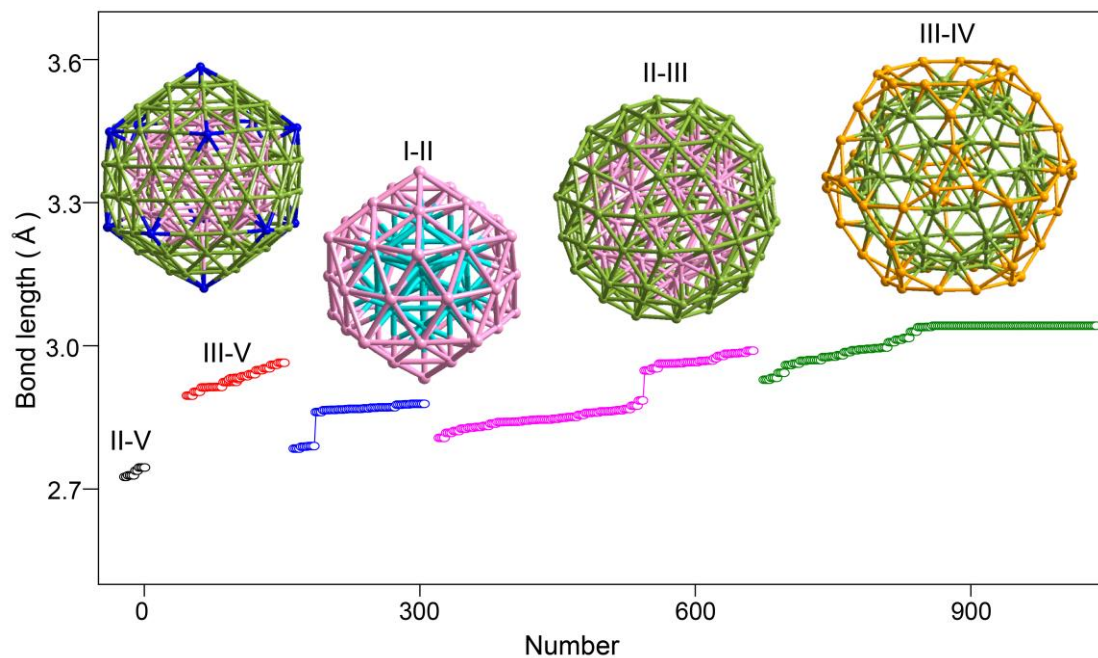
Supplementary Fig. 5 Molecular structure of $\text{Ag}_{135}\text{Cu}_{60}(\text{PET})_{60}\text{Cl}_{42}$ axial thickness dimensions were measured without considering the ligand shell.



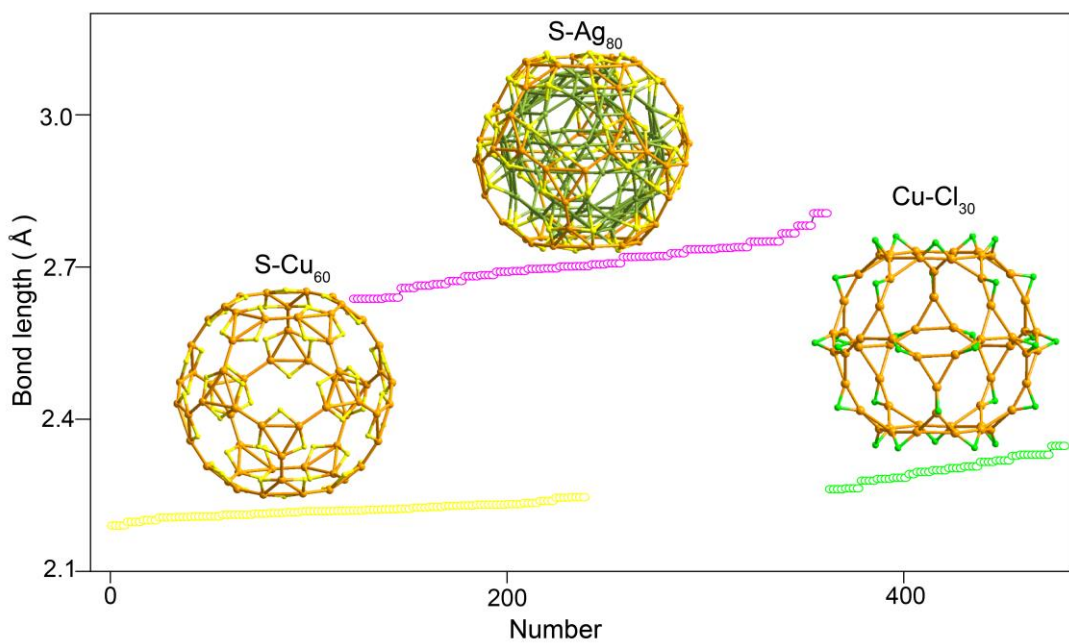
Supplementary Fig. 6 Monitoring the ambient stability of $\text{Ag}_{135}\text{Cu}_{60}$ in liquid state (a) and solid state (b), respectively, using UV-vis spectroscopy. Note, the solid is stored in a powdered state and then dissolved in dichloromethane after a certain period of time to measure the UV-vis spectrum.



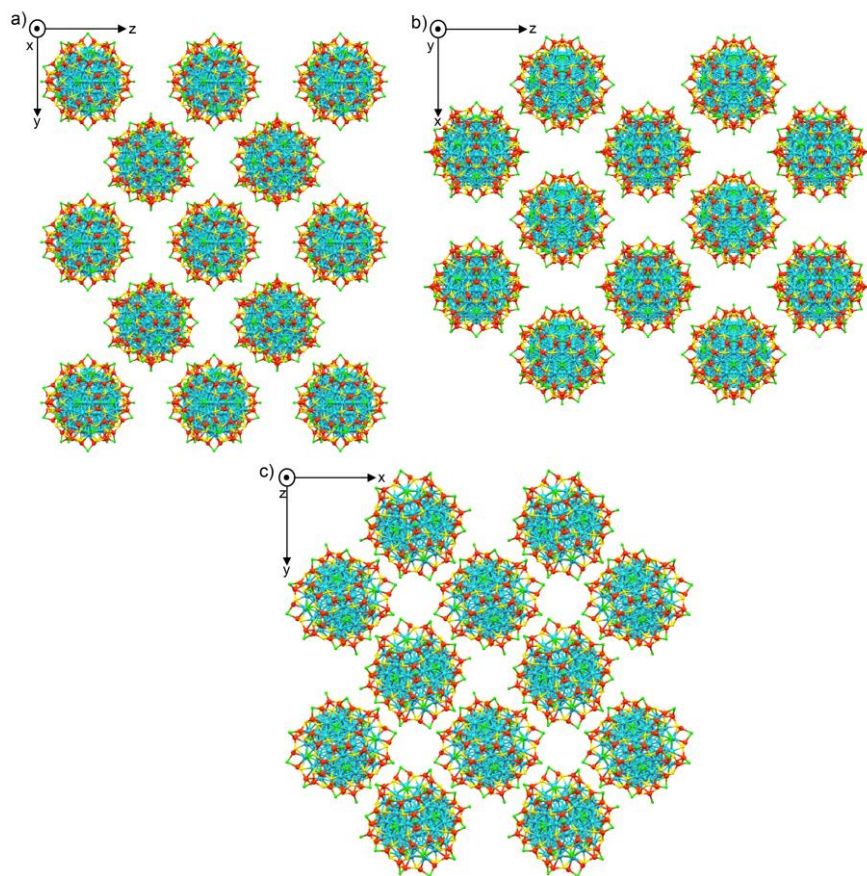
Supplementary Fig. 7 The distribution of bond lengths, shell by shell, in the $\text{Ag}_{135}\text{Cu}_{60}$ nanocluster. Note, the x-axis represents the number of lengths.



Supplementary Fig. 8 Lengths of bonds spread on between different layer of $\text{Ag}_{135}\text{Cu}_{60}$ nanocluster. Note, the x-axis represents the number of lengths.



Supplementary Fig. 9 The distribution of bond lengths of Cu-S, Ag-S, and Cu-Cl distances in in the $\text{Ag}_{135}\text{Cu}_{60}$ nanocluster. Note, the x-axis represents the number of lengths.



Supplementary Fig. 10 Packing of $\text{Ag}_{135}\text{Cu}_{60}(\text{SR})_{60}\text{Cl}_{42}$ nanoclusters in the crystal lattice: view from the x axis (a), y axis (b) and z axis (c). Color labels: turquoise = Ag; orange = Cu; yellow = S; green = Cl. All C and H atoms were omitted for clarity.

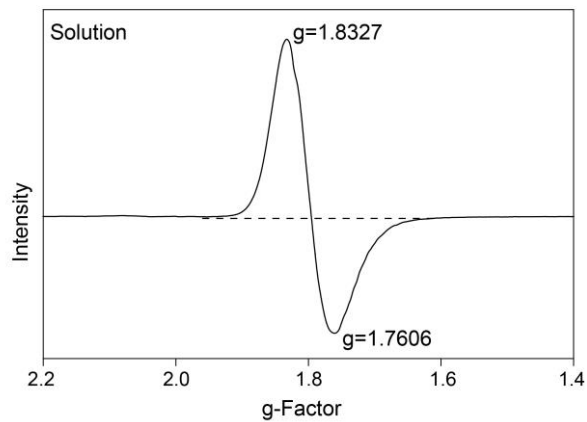
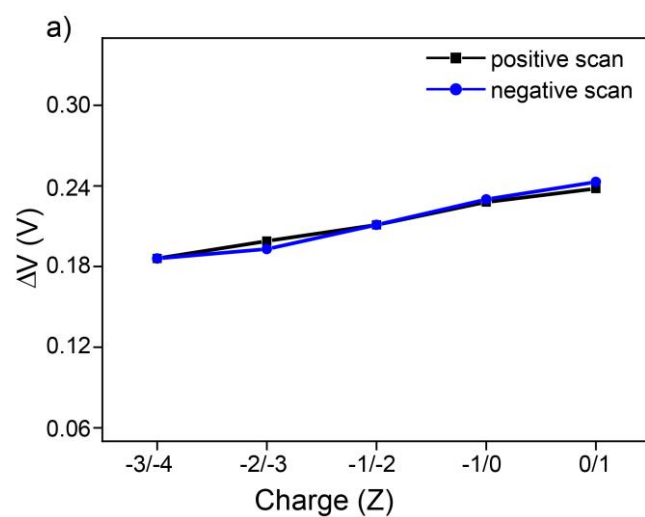
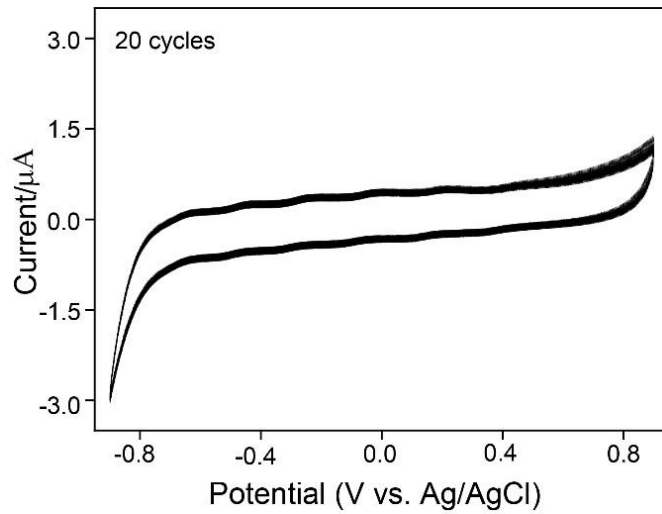


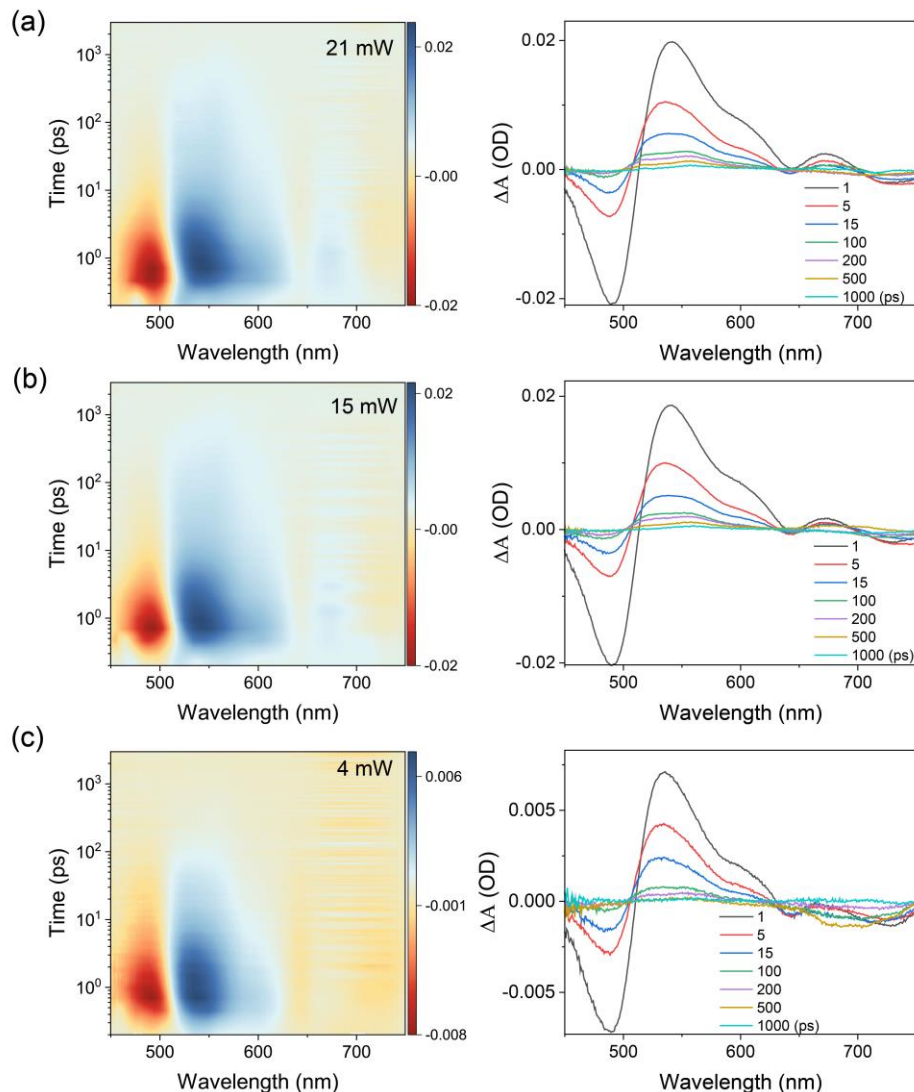
Figure S11. Electron paramagnetic resonance (EPR) spectra of $\text{Ag}_{135}\text{Cu}_{60}$ in solution state.



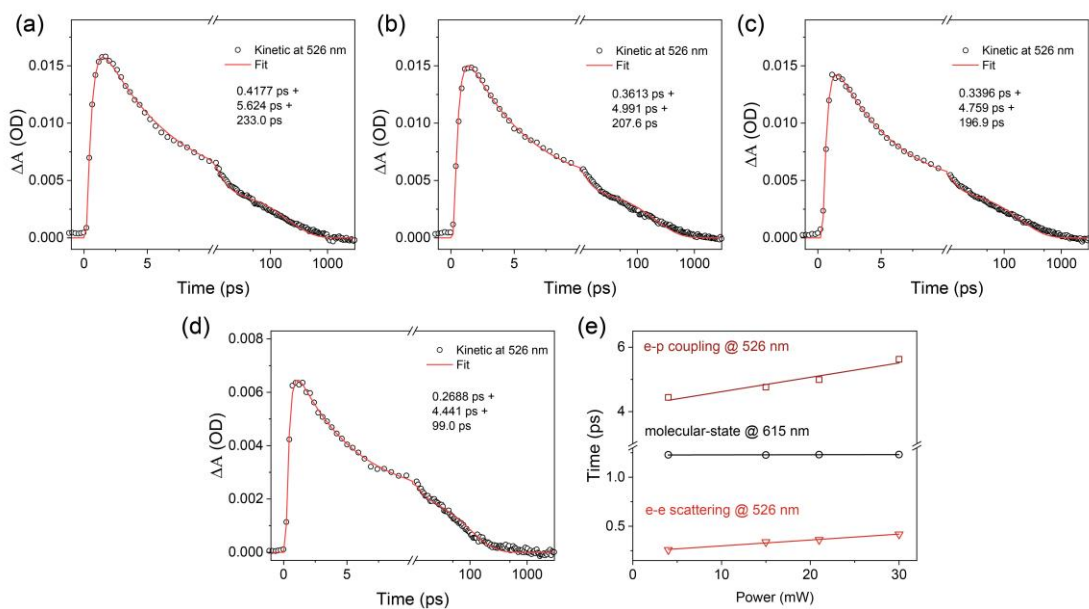
Supplementary Fig. 12 ΔV vs charge state plot revealing the peak spacing distribution for $\text{Ag}_{135}\text{Cu}_{60}$.



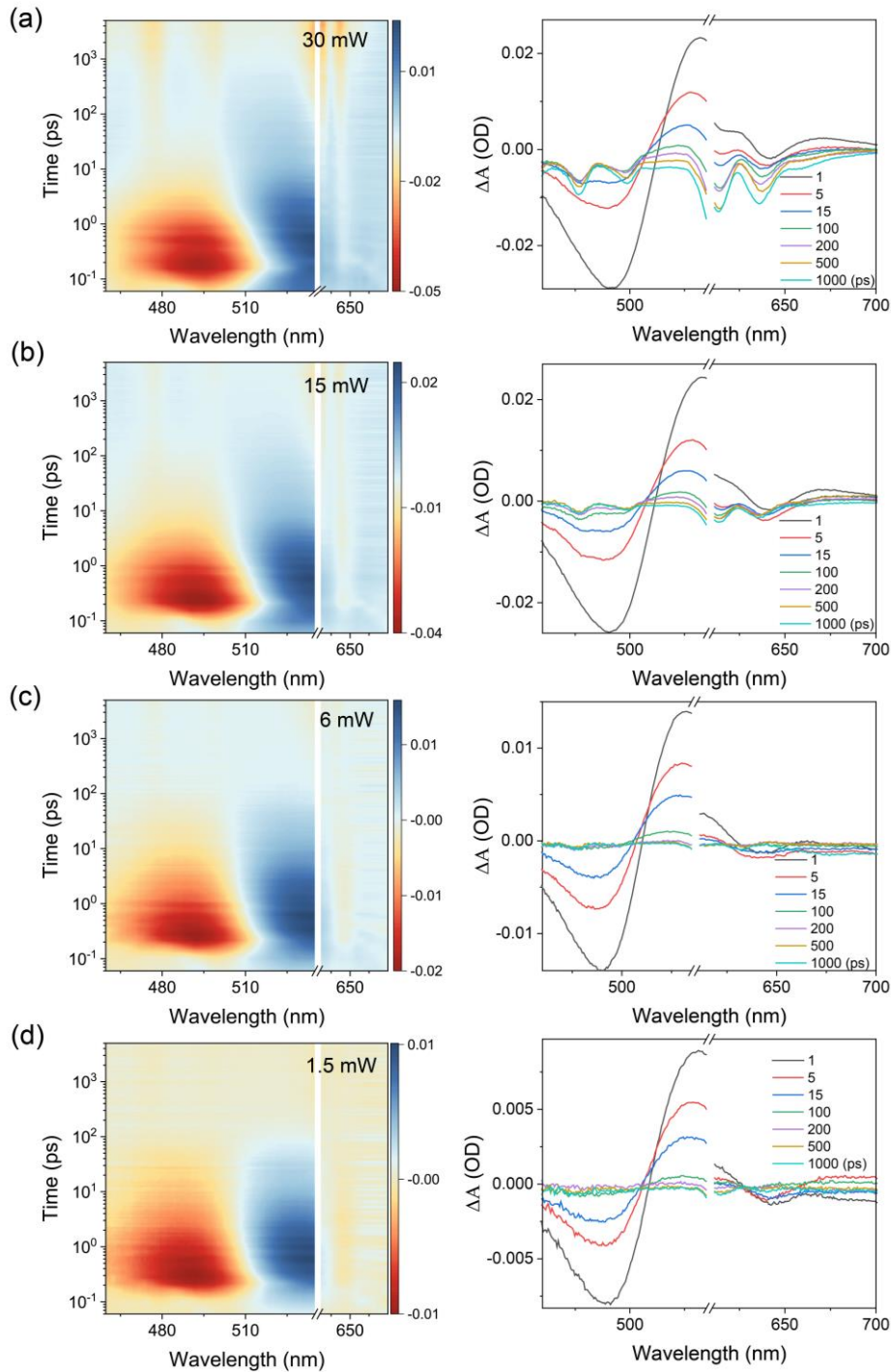
Supplementary Fig. 13 Cyclic voltammetry of $\text{Ag}_{135}\text{Cu}_{60}$ in CH_2Cl_2 containing 0.1 M Bu_4NPF_6 .



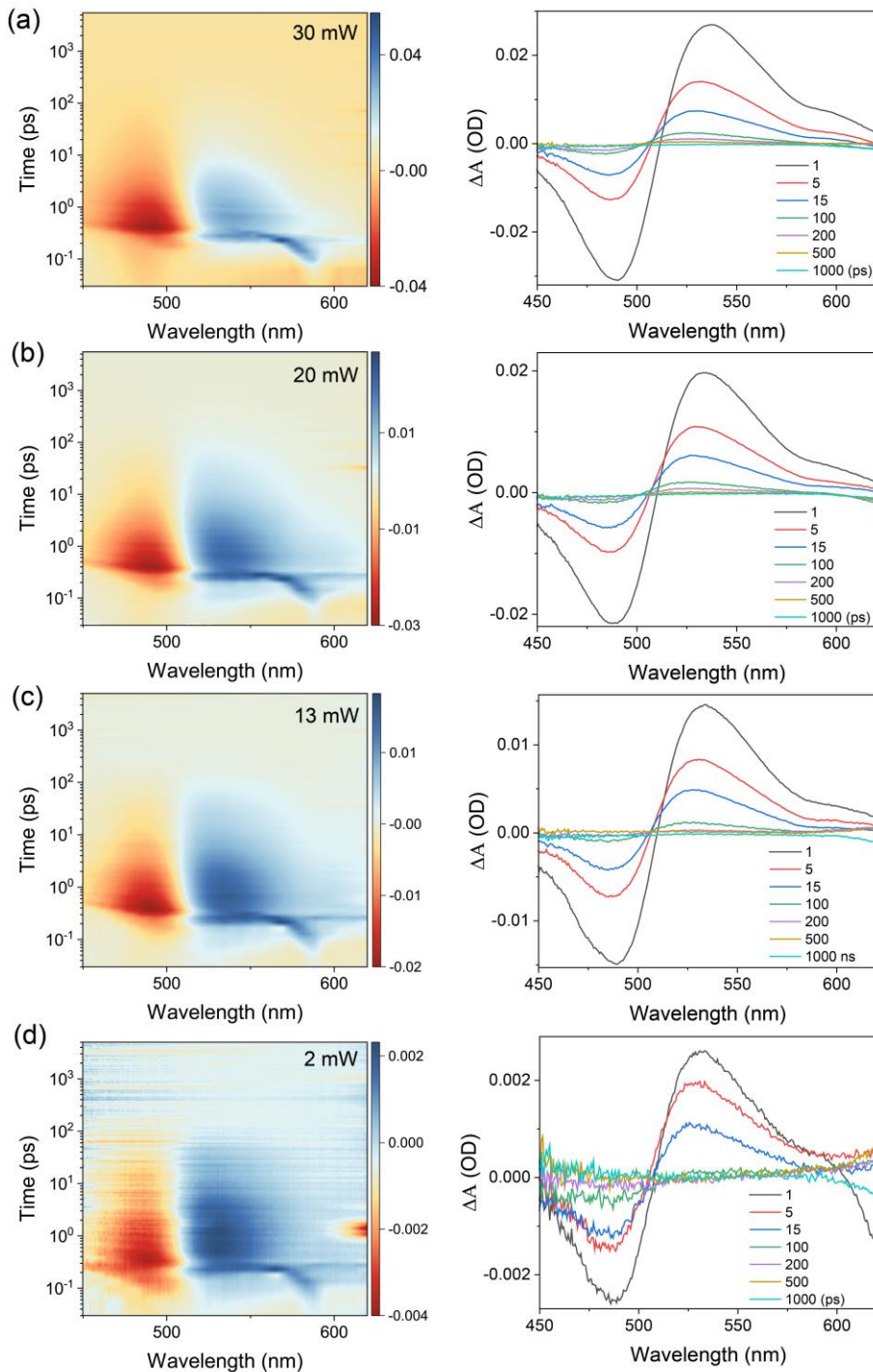
Supplementary Fig. 14 Femtosecond-TA maps and line-by-line TA spectra as a function of selected time delays from 1 ps to 1 ns under 365 nm excitation with pump power 21 mW (a), 15 mW (b), and 4 mW (c).



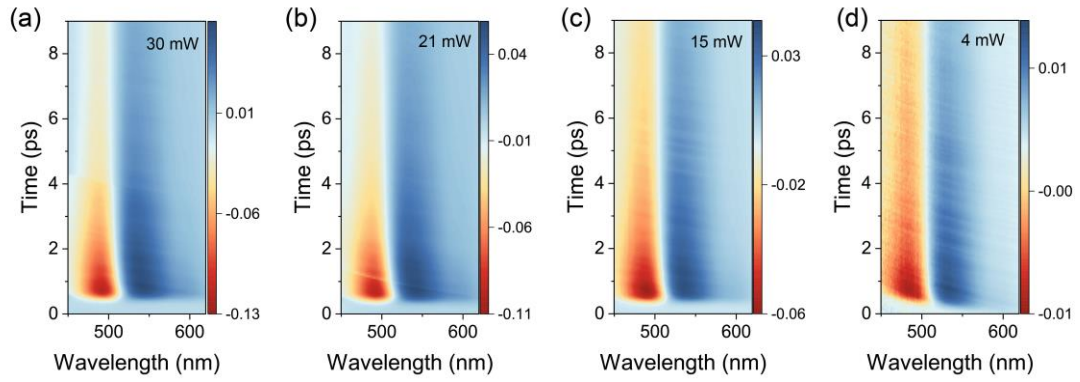
Supplementary Fig. 15 (a-d) Selected ESA kinetic decays at 526 nm for $\text{Ag}_{135}\text{Cu}_{60}$ NC upon 365 nm excitation with different pump powers and their corresponding fitting lines. (e) Relaxation time of $\text{Ag}_{135}\text{Cu}_{60}$ as a function of pump power.



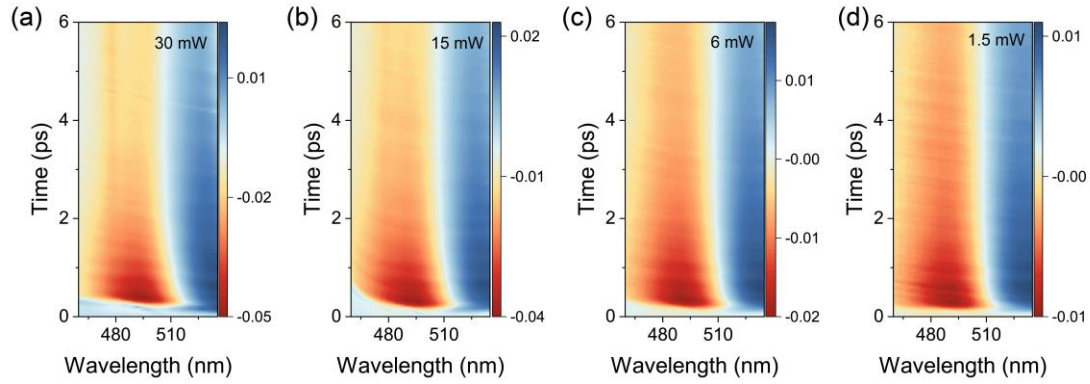
Supplementary Fig. 16 Femtosecond-TA maps and line-by-line TA spectra as a function of selected time delays from 1 ps to 1 ns under 570 nm excitation with pump power 30 mW (a), 15 mW (b), 6 mW (c) and 1.5 mW (d).



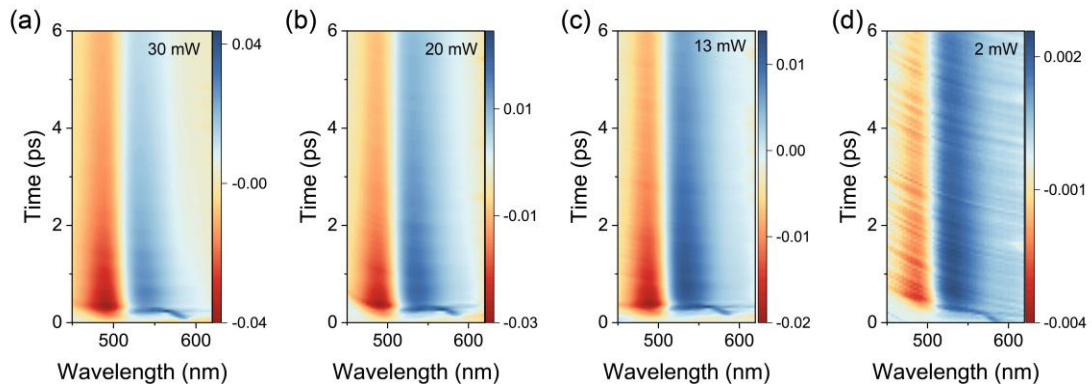
Supplementary Fig. 17 Femtosecond-TA maps and line-by-line TA spectra as a function of selected time delays from 1 ps to 1 ns under 680 nm excitation with pump power 30 mW (a), 20 mW (b), 13 mW (c) and 2 mW (d).



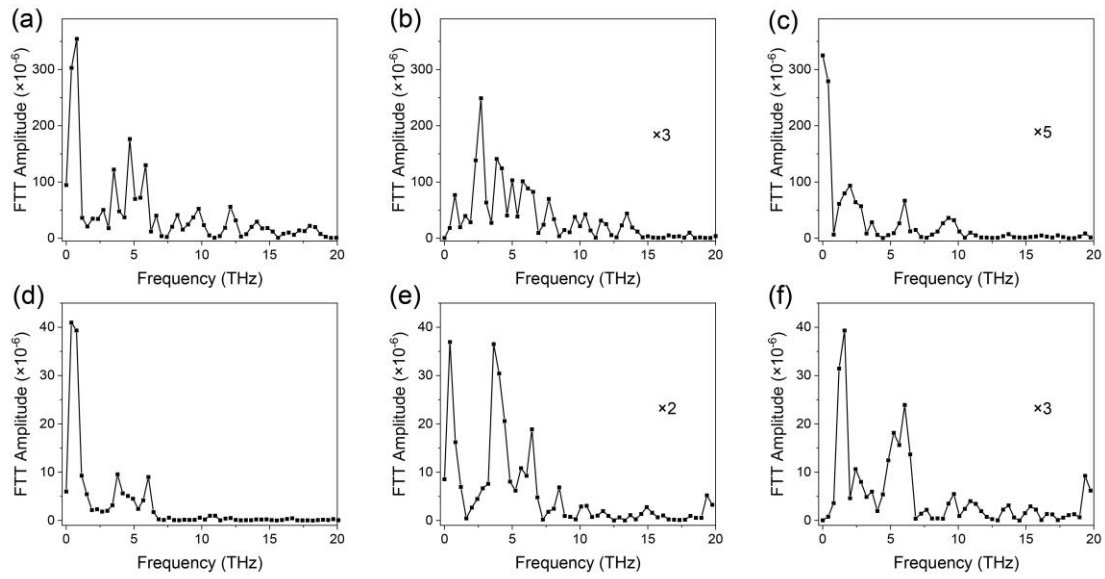
Supplementary Fig. 18 Femtosecond-TA maps within 9 ps upon 365 nm excitation with pump power 30 mW (a), 21 mW (b), 15 mW (c) and 4 mW (d).



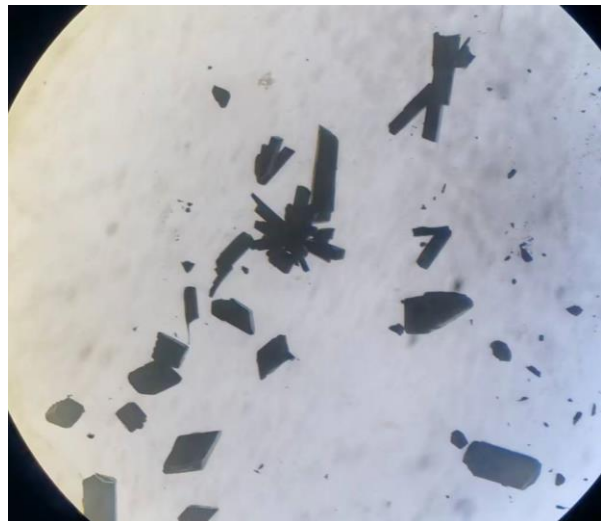
Supplementary Fig. 19 Femtosecond-TA maps within 6 ps upon 570 nm excitation with pump power 30 mW (a), 15 mW (b), 6 mW (c) and 1.5 mW (d).



Supplementary Fig. 20 Femtosecond-TA maps within 6 ps upon 680 nm excitation with pump power 30 mW (a), 20 mW (b), 13 mW (c) and 2 mW (d).



Supplementary Fig. 21 (a-c) Fourier transform results of the pure acoustic oscillations for $\text{Ag}_{135}\text{Cu}_{60}$ NC upon 570 nm excitation with pump powers 30 mW, 15 mW and 6 mW. (d-f) Fourier transform results of the pure acoustic oscillations in the inset for $\text{Ag}_{135}\text{Cu}_{60}$ NC upon 680 nm excitation with pump powers 30 mW, 20 mW and 13 mW.



Supplementary Fig. 22. Digital photo of single crystals of $\text{Ag}_{135}\text{Cu}_{60}$ clusters, which are grown by CH_2Cl_2 / *n*-Hex over 5-7 days.

Supplementary Tables 1-6

Supplementary Table 1 The atomic ratio of Ag and Cu in $\text{Ag}_{135}\text{Cu}_{60}$ was calculated from inductively coupled plasma (ICP), energy-dispersive X-ray spectrum (EDX) and X-ray photoelectric spectroscopy (XPS) measurements.

| Measurement | Ag(%) | Cu(%) |
|---------------------|----------------|---------------|
| ICP results | 69.1 | 30.9 |
| EDX results | 68.3 | 31.7 |
| XPS results | 68.5 | 31.5 |
| Theoretical results | 135/195 (69.2) | 60/195 (30.8) |

Supplementary Table 2. Crystal data and structure refinement for the $\text{Ag}_{135}\text{Cu}_{60}(\text{SR})_{60}\text{Cl}_{42}$ nanocluster. The CCDC number of the $\text{Ag}_{135}\text{Cu}_{60}(\text{SR})_{60}\text{Cl}_{42}$ nanocluster is 2307961.

| | |
|-----------------------------------------------|----------------------------------------------------------------------------------------|
| Molecular formula | $\text{C}_{480}\text{H}_{540}\text{Ag}_{135}\text{Cl}_{42}\text{Cu}_{60}\text{S}_{60}$ |
| Crystal system | Tetragonal |
| Space group | $\text{P}4_2/\text{m}$ |
| $a/\text{\AA}$ | 29.484(10) |
| $b/\text{\AA}$ | 29.484(10) |
| $c/\text{\AA}$ | 37.450(18) |
| $\alpha/^\circ$ | 90 |
| $\beta/^\circ$ | 90 |
| $\gamma/^\circ$ | 90 |
| Volume/ \AA^3 | 32556(27) |
| Z | 2 |
| $\rho_{\text{calc}}/\text{g/cm}^3$ | 2.886 |
| μ/mm^{-1} | 6.264 |
| $F(000)$ | 26358.0 |
| Radiation | $\text{MoK}\alpha (\lambda = 0.71073)$ |
| Index ranges | $-39 \leq h \leq 39, -38 \leq k \leq 37, -49 \leq l \leq 49$ |
| θ range ($^\circ$) | 3.778 to 56.386 |
| Measured reflections and unique reflections | 414419 / 40586 ($R_{\text{int}} = 0.0907, R_{\text{sigma}} = 0.0402$) |
| Goodness-of-fit on F^2 | 1.005 |
| Largest diff. peak/hole / $e \text{\AA}^{-3}$ | 2.74/-1.66 |
| Final R indexes [$ I \geq 2\sigma (I)$] | $R_1 = 0.0696, wR_2 = 0.1661$ |
| Final R indexes [all data] | $R_1 = 0.1199, wR_2 = 0.1988$ |

Supplementary Table 3. A summary of Ag-Ag distances in $\text{Ag}_{135}\text{Cu}_{60}$

| | Ag-Ag distance/ \AA | Average value/ \AA |
|-----------------------------|------------------------------|-----------------------------|
| 1st shell: Ag_{13} | 2.765-2.916 | 2.868 |
| 2nd shell: Ag_{42} | 2.905-3.004 | 2.952 |
| 3rd shell: Ag_{80} | 2.869-3.092 | 2.973 |
| 5th shell: Cu_{60} | 2.900-3.648 | 3.313 |

Supplementary Table 4. A summary of between different layer distances in $\text{Ag}_{135}\text{Cu}_{60}$.

| | Bond distance/Å | Average value/Å |
|------------------------------------------------------------|-----------------|-----------------|
| 4th shell: $\text{Cl}_{12}-\text{Ag}_{42}$ | 2.725-2.744 | 2.734 |
| 4th shell: $\text{Cl}_{12}-\text{Ag}_{60}$ | 2.895-2.964 | 2.930 |
| 1st and 2nd: $\text{Ag}_{13}-\text{Ag}_{42}$ | 2.784-2.878 | 2.856 |
| 2nd and 3rd: $\text{Ag}_{42}-\text{Ag}_{80}$ | 2.806-2.989 | 2.873 |
| 3rd and Cu_{60} : $\text{Ag}_{80}-\text{Cu}_{60}$ | 2.928-3.437 | 3.107 |

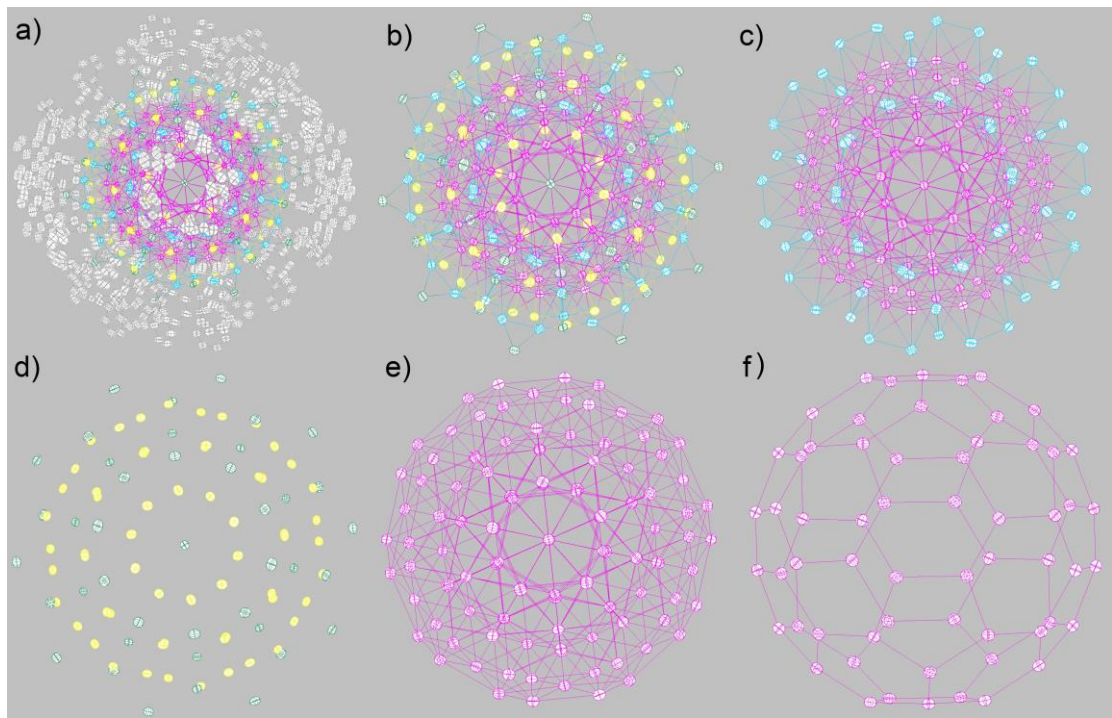
Supplementary Table 5. A summary of bond lengths of Cu-S, Ag-S, and Cu-Cl distances in $\text{Ag}_{135}\text{Cu}_{60}$.

| | Bond distance/Å | Average value/Å |
|------------------------------------|-----------------|-----------------|
| Cg-S: $\text{Cu}_{60}-\text{S}$ | 2.190-2.246 | 2.219 |
| Ag-S: $\text{Ag}_{60}-\text{S}$ | 2.637-2.805 | 2.707 |
| Cu-Cl : $\text{Cu}-\text{Cl}_{30}$ | 2.262-2.347 | 2.301 |

Supplementary Table 6. The DPV response peaks in the entire potential window of -0.9 V - 0.9 V.

| | Positive | | | Negative | |
|------------------------|---------------|----------------|--------------|---------------|----------------|
| Charge state | Potential (V) | ΔV (V) | Charge state | Potential (V) | ΔV (V) |
| -3/-4 (R_4) | -0.726 | 0.186 | -3/-4 | -0.687 | 0.185 |
| -2/-3 (R_3) | -0.540 | 0.199 | -2/-3 | -0.502 | 0.194 |
| -1/-2 (R_2) | -0.341 | 0.211 | -1/-2 | -0.308 | 0.211 |
| -1/0 (R_1) | -0.130 | 0.228 | -1/0 | -0.097 | 0.230 |
| 0/1 (O_1) | 0.098 | 0.238 | 0/1 | 0.133 | 0.243 |
| 1/2 (O_2) | 0.336 | | 1/2 | 0.376 | |

ORTEP view of $\text{Ag}_{135}\text{Cu}_{60}$ nanocluster



ORTEP view of $\text{Ag}_{135}\text{Cu}_{60}$ nanocluster at 30% probability level. a) Total structure (excluding hydrogen atoms); b) The structure after removal of carbon atoms; c) The structure with all non-metal atoms removed; d) The structure of non-metal atoms; e) The structure of silver kernel; f) The structure of the Ag_{60} framework. Atoms are color-coded: carbon (white), chlorine (green), sulfur (yellow), copper (cyan) and silver (magenta) to differentiate between elements in the structure.

Explanations for A and B alerts in $\text{Ag}_{135}\text{Cu}_{60}$ nanocluster structure

A and B alerts mainly indicate "Check Calculated Positive Residual Density on Ag." In reality, there are no elements heavier than silver (Ag) in the molecule. Therefore, the residual peaks around Ag are caused by Fourier truncation.

Alert level A

PLAT973_ALERT_2_A Check Calcd Positive Resid. Density on Ag1 3.12 eA-3

Author Response: the residual peaks around Ag are caused by fourier truncation

PLAT973_ALERT_2_A Check Calcd Positive Resid. Density on Ag6 2.77 eA-3

Author Response: the residual peaks around Ag are caused by fourier truncation

PLAT973_ALERT_2_A Check Calcd Positive Resid. Density on Ag11 2.76 eA-3

Author Response: the residual peaks around Ag are caused by fourier truncation

PLAT973_ALERT_2_A Check Calcd Positive Resid. Density on Ag4 2.66 eA-3

Author Response: the residual peaks around Ag are caused by fourier truncation

PLAT973_ALERT_2_A Check Calcd Positive Resid. Density on Ag31 2.50 eA-3

Author Response: the residual peaks around Ag are caused by fourier truncation

PLAT973_ALERT_2_A Check Calcd Positive Resid. Density on Ag8 2.50 eA-3

Author Response: the residual peaks around Ag are caused by fourier truncation

PLAT973_ALERT_2_A Check Calcd Positive Resid. Density on Ag15 2.47 eA-3

Author Response: the residual peaks around Ag are caused by fourier truncation

PLAT973_ALERT_2_A Check Calcd Positive Resid. Density on Ag12 2.45 eA-3

Author Response: the residual peaks around Ag are caused by fourier truncation

PLAT973_ALERT_2_A Check Calcd Positive Resid. Density on Ag29 2.44 eA-3

Author Response: the residual peaks around Ag are caused by fourier truncation

PLAT973_ALERT_2_A Check Calcd Positive Resid. Density on Ag18 2.41 eA-3

Author Response: the residual peaks around Ag are caused by fourier truncation

PLAT973_ALERT_2_A Check Calcd Positive Resid. Density on Ag16 2.22 eA-3

Author Response: the residual peaks around Ag are caused by fourier truncation

PLAT973_ALERT_2_A Check Calcd Positive Resid. Density on Ag25 2.22 eA-3

Author Response: the residual peaks around Ag are caused by fourier truncation

PLAT973_ALERT_2_A Check Calcd Positive Resid. Density on Ag13 2.19 eA-3

Author Response: the residual peaks around Ag are caused by fourier truncation

PLAT973_ALERT_2_A Check Calcd Positive Resid. Density on Ag36 2.08 eA-3

Author Response: the residual peaks around Ag are caused by fourier truncation

PLAT973_ALERT_2_A Check Calcd Positive Resid. Density on Ag20 2.06 eA-3

Author Response: the residual peaks around Ag are caused by fourier truncation

Alert level B

PLAT910_ALERT_3_B Missing # of FCF Reflection(s) Below Theta(Min). 15 Note

0 1 0, 1 1 0, -1 2 0, 0 2 0, 1 2 0, 0 1 1,

1 1 1, -1 2 1, 0 2 1, 1 2 1, 0 0 2, 0 1 2,

1 1 2, 0 2 2, 0 1 3,

Author Response: some reflections are blocked by beamstop due to the large unit cell

PLAT973_ALERT_2_B Check Calcd Positive Resid. Density on Ag22 1.98 eA-3

Author Response: the residual peaks aroudn Ag are casued by fourier

tuncationPLAT973_ALERT_2_B Check Calcd Positive Resid. Density on Ag33 1.96 eA-3

Author Response: the residual peaks aroudn Ag are casued by fourier tuncation

PLAT973_ALERT_2_B Check Calcd Positive Resid. Density on Ag35 1.96 eA-3

Author Response: the residual peaks aroudn Ag are casued by fourier tuncation

PLAT973_ALERT_2_B Check Calcd Positive Resid. Density on Ag27 1.90 eA-3

Author Response: the residual peaks aroudn Ag are casued by fourier tuncation

PLAT973_ALERT_2_B Check Calcd Positive Resid. Density on Ag19 1.89 eA-3

Author Response: the residual peaks aroudn Ag are casued by fourier tuncation

PLAT973_ALERT_2_B Check Calcd Positive Resid. Density on Ag24 1.85 eA-3

Author Response: the residual peaks aroudn Ag are casued by fourier tuncation

PLAT973_ALERT_2_B Check Calcd Positive Resid. Density on Ag37 1.85 eA-3

Author Response: the residual peaks aroudn Ag are casued by fourier tuncation